Cross-linked poly(4-vinylpyridine) particles for pH- and ionic strength-responsive "on–off" Pickering emulsions

Grégory Douyère, Loïc Leclercq, Véronique Nardello-Rataj

Cross-linked poly(4‑vinylpyridine) particles for pH- and ionic strength-responsive "on-off" Pickering emulsions

Grégory Douyère, Loïc Leclercq,* Véronique Nardello-Rataj

Univ. Lille, CNRS, Centrale Lille, Univ. Artois, UMR 8181-UCCS, Unité de Catalyse et Chimie du Solide, 59000 Lille, France. E-mail: loic.leclercq@univ-lille.fr

Abstract.

Poly(4-vinylpyridine) particles, P4VP, show a great potential from the environmental and economic perspective since they are cheap and extensively used for safer and greener organic syntheses. Moreover, their pH-sensitive properties would make it easy to obtain "on-off", recyclable and reusable Pickering emulsions. The relationships between the particles structures (size, shape, acidity and charge) and the emulsions properties (type, droplet size and stability against environmental stresses) were investigated. The protonation increased the particles diameter to 147 nm compared to the pristine ones (88 nm) due to electrostatic repulsions which swell the particles. The ζ-potential was decreased with increasing acidity (from +60 to +30 mV) due to the accumulation of chlorides onto the surface. Thus, the acidic particles of 39 mmolH$^+$/g and +57 mV were more effective in emulsifying heptane in water with long-term stability in storage conditions (up to one year) and unprecedented resistance against centrifugation and temperature (up to 5,000 rpm and 60 °C). Nevertheless, destabilization can be easily achieved by pH or ionic strength changes facilitating the phase separation and the particles recovery. Contrary to the literature of responsive Pickering emulsions, which require relatively complex systems, the investigated one provides a simple route to obtain various "on-off" switches using P4VP cross-linked particles which possess changeable structures based on electrostatic repulsions. Consequently, the exploitation of such a system could be attractive in biphasic media in which the P4VP would act as a reagent, scavenger, and/or catalyst.

1. Introduction

Pickering emulsions have aroused considerable interest due to their role in numerous industrial processes and products (*e.g.* agriculture [1], food [2], pharmacy [3], cosmetic [4], medicine [5], *etc.*). This broad interest is mainly linked to the solid particles absorbed on the water/oil interfaces leading to the formation of a dense film preventing coalescence and conferring long-term stability and a reduction of foaming during emulsion preparation [6]. Moreover, unlike molecular surfactants which have a substantial negative impact on ecosystems and require large amounts to produce stable emulsions, Pickering emulsifiers are considered to be more eco-friendly and cost-saving [7]. In this context, a wide variety of native or modified particles have served as Pickering emulsifiers (*e.g.* silica [8], clay [9], metal oxide [10], carbon [11], proteins [12], polysaccharides [13], cyclodextrins [14], supracolloids [15] or polymers [16]). Unfortunately, the high-stability of Pickering emulsions is sometimes unsuitable for specific applications, such as controlled release [17], emulsion polymerization [18] or catalysis [19]. In these cases, stimulus-responsive Pickering emulsions may be required to switch between long-term stability and rapid phase separation through appropriate environmental triggers (*e.g.* temperature, pH, ionic strength, magnetic field, *etc.*) [20].

In the past decades, the emulsions stabilized by microgel particles have attracted much attention [21]. From a theoretical point of view, they are crosslinked polymer-based particles forming a 3D network that allow, in an appropriate solvent, a transition between swollen and shrunk particles by adjusting the temperature, pH and/or the ionic strength [22]. This behavior offers an unprecedented degree of control on the resulting emulsions although an amphiphilic balance remains an essential requirement as for those that use molecular surfactants or conventional solid particles [23,24]. For this purpose, the copolymers allows a judicious combination of hydrophilic and hydrophobic block with appropriate environmental triggers [25]. Thus, poly(*N*-isopropylacrylamide), PNIPAM, or poly(*N*-isopropylmethacrylamide), PNIPMAM, can be used as thermo-responsive part. For instance, P(NIPAM-*co*-NIPMAM) and P(NIPAM)-P(NIPMAM) microgels provide emulsions which can be broken by increasing the temperature above the volume phase transition temperature [26]. In contrast,

2

pH-sensitive copolymer-based microgels use a polyacid or a polybase block (*e.g.* poly(methacrylic acid), PMAA, or poly(4-vinylpyridine), P4VP) copolymerized with NIPAM, styrene, *etc.* [27]. For instance, the microgels based on P4VP/silica colloidal nanocomposite particles readily provide emulsions at high pH value as the surface of particles consists of hydrophilic silica and hydrophobic P4VP chains [28]. Note that ethylene glycol dimethacrylate is used as cross-linker to avoid particle dissolution. Nevertheless, the phase separation is easily ensured by the swelling of microgels due to the P4VP protonation. In addition to the pH, the degree of ionization also influences the stabilization of these emulsions [22]. From a similar mechanism, pH-responsive emulsions can be obtain from Au@poly(ethylene oxide-*b*-4-vinylpyridine) polymer-metal hybrid micelles [29]. However, the crosslinking of the polymer micelle core was necessary to avoid the polymer micelles dissociation and to allow reversible emulsification/demulsification cycles with pH variation. Unfortunately, all these previous particles require synthetic steps before use (*e.g.* (co)polymerization, cross-linking, grafting, functionalization, *etc.*) [30-33]. Consequently, they fail to provide ideal responsive emulsions which should be directly stabilized by cheap commercially available particles without any chemical transformation. We are clearly surprised of this finding because commercial P4VP particles, crosslinked with divinylbenzene (DVB), which nevertheless seem to be ideal to obtain inexpensive responsive emulsions, are, to our knowledge, omitted from the literature. Moreover, it is noteworthy that crosslinked P4VP are widely used as a reagent, scavenger, and/or catalyst for safer and greener syntheses due to their solid nature and easy recovery [34].

As "*simplicity is the ultimate sophistication*" (quote attributed to Leonardo da Vinci), we report the use of commercial crosslinked P4VP particles to easily provide Pickering emulsions. As these native particles are too hydrophobic to stabilize emulsions, their charge density was adjusted by protonation (Figure 1). In this work, we particularly focus our attention on the relationships between the protonated particles structures (size, shape, degree of protonation and charge) and the emulsions properties (type of emulsion, droplet size, and stability against storage conditions and against environmental stresses such as pH and temperature). The as-prepared emulsions showed very high

stability but can be easily destabilized by pH or ionic strength changes leading to phase separation and particles recovery (switching service, see Figure 1).
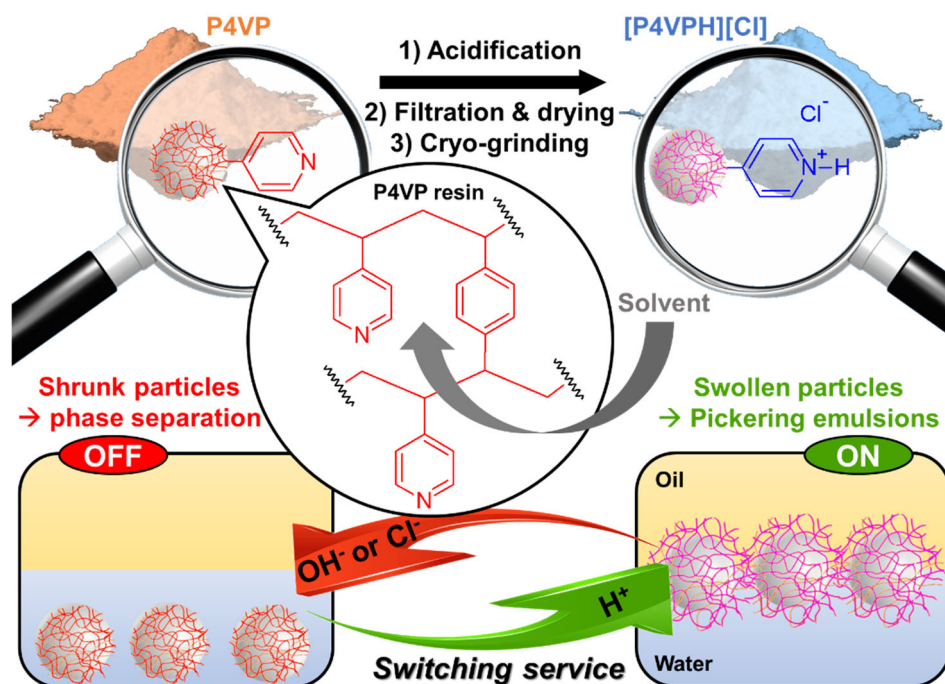

Figure 1. Poly(4-vinylpyridine) colloidal particles crosslinked with divinylbenzene (P4VP, top) and concept of responsive emulsions as a function of charge density and solvent penetration (bottom).

2. Experimental section

2.1. Materials and general information

The native P4VP (2% cross-linked with DVB) was purchased from Sigma-Aldrich. Prior to use, the P4VP was cryo-grinded (MM400, Retsch, Germany). It was placed in two 25 mL stainless steel grinding bowls filled with: 1/3 of P4VP, 1/3 of 5 mm-diameter stainless steel balls and 1/3 of air. The bowls were immersed into liquid nitrogen for 4 minutes and grinded at a frequency of 30 s^{-1} for 30 min. Water was purified using a water purification system (Barnstead, Thermo Scientific, USA) with a resistivity higher than 18.2 MΩ cm. The other chemicals were obtained from Sigma-Aldrich with the highest purity and used without further purification. To ensure repeatability, physicochemical measurements were performed three times. pH was determined with pH330i (WTW, Germany). Conductivity was measured with a CDM210 (Radiometer Analytical, France). Centrifugation experiments were performed with a Sigma 2-16PK apparatus (20 min at 5,000 rpm).

2.2. Preparation of particles

Partially protonated P4VP particles were prepared by adding 500 mg of cryo-grinded native P4VP into 50 mL aqueous solutions of hydrochloric acid at different concentrations (5×10^{-3}, 10^{-2}, 2.5×10^{-2}, 5×10^{-2}, 7.5×10^{-2}, 0.1, 0.5 and 2 M). The solutions were then stirred at 500 rpm for 4 h. The particles were then filtrated, dried overnight and cryo-grinded before characterization (see section 2.1).

2.3. Characterization of particles

Fourier transform infrared spectroscopy (FTIR) was carried out with a Nicolet 380 FTIR Spectrometer equipped with an attenuated total reflector (Thermo Electron, USA). Thermogravimetric analyses were carried out on a Q500 (TA Instruments, USA). About 10 mg of product were heated from 25 to 500 °C at a rate of 10 °C/min under nitrogen atmosphere (60 mL/min). To measure the acidity of particles, 500 mg of each acidified P4VP particles were dispersed into in NaCl aqueous solution (50 mL at 0.5 M) at room temperature and stirred overnight. Then, the solid was filtered off and the resulting solution was titrated with a NaOH solution (from 10 mM) using a pH-meter. The particle size distribution was determined by dynamic light scattering (DLS) with the Zetasizer Nano ZS ZEN 3600 (Malvern, UK). An automatic process was performed at 173° with a 10-runs method providing time-correlation functions. Data were analyzed by cumulating analysis to obtain an average diffusion coefficient used to calculate a hydrodynamic radius using the Stokes-Einstein equation. The ζ-potential was also measured after dispersing the particles into water (or in 1:1 water/ethanol mixture or heptane) at 25 °C. An automatic process was performed with a series of 10 to 100 measurements maximum for each sample. The morphology of the particles was inspected by scanning electron microscopy (SEM) using a JSM-7800F LV (Jeol, Japan) operating at 5 kV. One drop of the particles dispersed in water was deposited onto a carbon conductive adhesive tape stuck on a stub (1.3 cm radius) and the observations were performed after the evaporation of water by air-drying and chromium coating. The transmission electron microscopy (TEM) micrographs were obtained on a TECNAI G2-20 Twin microscope (FEI, USA), equipped with a LaB6 filament operating at 200 kV. Two drops of nanoparticles suspension were deposited on a carbon-copper grid

(CF200-Cu, Electron Microscopy Sciences, USA). The contact angles (θ) were measured according to the spreading method. The P4VP particles were compressed at 1,800 bars pressure during 1 min and the contact angles were determined by using drop shape analyzer DSA 100 (Krüss GmbH, Germany) by depositing 4 µL of solvent (glycerol or paraffin oil) onto the compressed particles. The stability of particles aqueous dispersions was quantified at 25 °C by static multiple light scattering using a Turbiscan Lab (Formulaction, France) operating using a near-infrared light source ($\lambda = 880$ nm).

2.4. Emulsion preparation

Water and particles (47.5 and 5 wt.%, respectively) were weighted in a glass vial ($\emptyset = 16$ mm; H = 60 mm) before adding heptane (47.5 wt.%). The emulsification was performed using a T10 basic Ultraturrax (IKA, Germany, 11,500 rpm, 60 s).

2.5. Emulsion characterization

The type of emulsion was determined by electric conductivity measurement. Optical microphotographs were obtained using a VHX-900F digital microscope equipped with a VH-Z100UR/W/T lens (Keyence, France). The log-normal distribution function was obtained after statistical analysis of the microphotographs using OriginPro 8® (OriginLab, USA). The morphology of the emulsions was also inspected by SEM after the evaporation of water and heptane-core by air-drying (see above). The stability of emulsions was evaluated at 25 °C using the Turbiscan (see section 2.3) over 2 days. The rheological properties were evaluated using a Kinexus (Malvern, UK) equipped with a 20 mm-diameter plane geometry cone mobile imposing a logarithmic stress ramp increase followed by a reverse stress decrease from 0 to 500 Pa. The temperature was controlled using a Peltier temperature control device (± 0.01 °C).

2.6. Emulsion destabilization

3 mL of emulsion were introduced into a glass vial ($\emptyset = 16$ mm; H = 60 mm). 0.2 mL of aqueous HCl (5 M), aqueous NaOH (5 M) or 0.5 mL of aqueous NaCl (0.5 M; 0.5 mL) were then added. The resulting emulsions were then kept at room temperature overnight.

3. Results and discussion

As native P4VP, which contains 2% DVB, is too hydrophobic, it does not naturally stabilize emulsions. However, the presence of pyridine residues makes it possible to protonate it in an acidic medium, which makes it possible to counterbalance the excessively hydrophobic nature of P4VP (see Figure 1). As pH modification results in changes in the degree of ionization of surface groups, the isoelectric point (IEP), defined as the pH value at which the particles carry no net electrical charge, is a key parameter to obtain stable systems. Indeed, the condition of lowest stability, frequently leading to aggregation and precipitation for suspensions and to phase separation for emulsions, is obtained near the IEP. For the P4VP particles, the pyridine sidechains vary from charged at $pH < pK_a$ to uncharged at high pH. As the exact pH dependence depends on the surface chemistry, a pH titration can be used to determine the IEP of the commercial P4VP particles. An indirect estimation of the particle surface charge is the measurement of the ζ-potential. In short, ζ-potential is the electric potential at the slipping plane, *i.e.* the potential difference between the dispersion medium and the stationary layer of fluid attached to the dispersed particles. Thus, particles dispersed in a solvent can be negatively or positively charged according to particle size, effective charge on the surface, and solution chemistry (*e.g.* pH, electrolyte concentration). In respect with this, a dispersion of commercial P4VP in deionized water was prepared at pH 2.3 and a titration with NaOH was subsequently used to measure ζ-potential as a function of pH (Figure 2). At low pH, there is an excess of positively charged pyridines, leading to a positive ζ-potential (up to $+34 \pm 4$ mV at pH 2.3). As pH is raised further, the protons are removed, leading to a decrease of the ζ-potential until to reach an average surface charge of zero at pH 5.1. Above pH 5.1, the P4VP is fully deprotonated but a more and more negative ζ-potential is observed. This observation can be related to a strong prevalence of OH^- ions at the slipping plane, leading to negative ζ-potentials over the basic pH range (up to -47 ± 5 mV at pH 11.6). Indeed, as the ζ-potential is governed by not only the surface chemistry but also by the surrounding medium, we can suppose that the negative net surface charge arises from adsorption of OH^- ions onto the P4VP particles surface. The IEP is obtained at pH 5.1 which is in

7

good agreement with the pK_a values of 4-vinylpyridine (5.62) [35] and P4VP (~5) [36]. As a ζ-potential value outside the range -30 to +30 mV usually refers to the ability to resist aggregation, flocculation and coagulation (*i.e.* electrostatic repulsions are sufficient to overcome van der Waals attractive forces), the P4VP aqueous dispersions are stable below pH 2.3 and above 8.5.
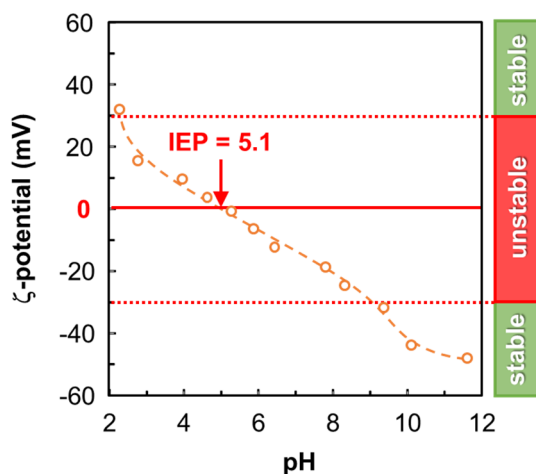

Figure 2. Titration of commercial P4VP (2% DVB) aqueous dispersion (0.05 wt.% in deionized water) using ζ-potential (S.D. ± 10%) as a function of pH (IEP = isoelectric point).

Based on the previous titration curve and as a ζ-potential greater than +30 mV is required to obtain good physical stability of suspensions and/or emulsions, various protonated P4VP particles ([P4VPH][Cl]) were prepared by dispersion of native P4VP into aqueous solutions of HCl at different concentrations for which the pH values are less than 2.3 (see Figure 1). Along with pH values, the contact time also affects the [P4VPH][Cl] preparation. Indeed, at the instant particles are dispersed in the aqueous HCl solution, protons begin to diffuse and adsorb at the newly created solid/liquid interface. It takes some time to reach equilibrium. This is why the contact time is fixed at 4 hours to achieve the maximal protonation of accessible pyridine units regardless of the pH (*i.e.* the HCl concentration). After drying and cryo-grinding, particles were characterized by their acidity (expressed in the form of acid density; mmolH$^+$/g) and by their average hydrodynamic diameter (obtained by dynamic light scattering, DLS, see Figure 3A). In addition, Fourier transform infrared spectroscopy (FTIR) and thermogravimetric analyses were also performed (Figures 3B and C, respectively). For reference purpose, the pristine P4VP follows similar preparation to the

8

[P4VPH][Cl] ones but was suspended in distilled water (*i.e.* with HCl = 0 M). Not surprisingly, the particles acidity can be easily adjusted: the maximal protonation capacity was found to be 112 mmol H$^+$ per gram of P4VP particles (Figure 3A). The interaction between hydrochloric acid and P4VP particles was confirmed by FTIR analysis. Indeed, the presence of the pyridinium ring increases the number of vibrational modes and brought completely different FTIR spectra as a result of change in the force constants with the protonation [37].
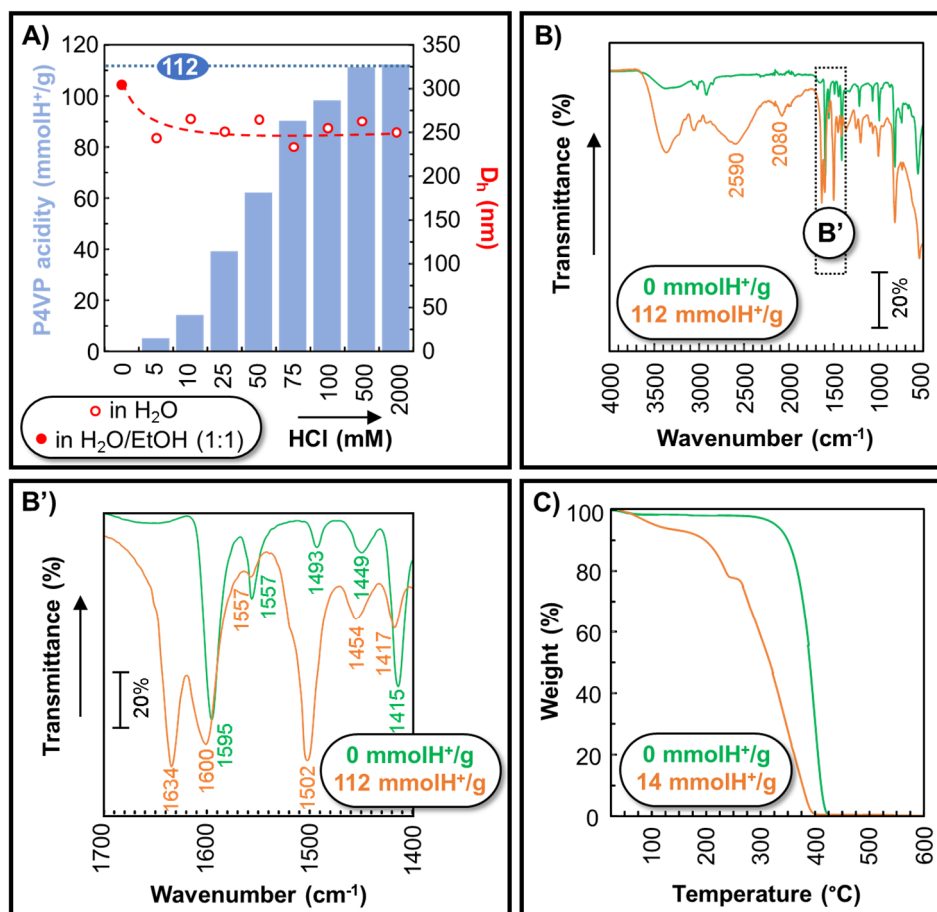

Figure 3. Acidity (S.D. ± 5%) and hydrodynamic diameter (D$_h$, S.D. ± 7%) of isolated protonated P4VP particles as a function of HCl concentration used for their preparation (**A**), typical FTIR spectra and thermogravimetric curves (**B** and **C**, respectively).

The C-H valency vibrations of the polymer chain and of the side groups appear in the 3200-2700 cm^{-1} region and undergo practically no change with the protonation. In contrast, in the 2700-2000 cm^{-1} region, the apperance of broad peaks near 2080 and 2590 cm^{-1} are observed for [P4VPH][Cl] due to the N$^+$-H valency vibrations of pyridinium residues. The valency and deformation vibrations of the

9

pyridine or pyridinium rings appear in the 2000-400 cm^{-1} region. For instance, peaks near 1595, 1557, 1493, 1449, and 1415 cm^{-1} correspond to the stretching vibrations of the pyridine ring of P4VP. The frequencies of these bands are displaced with the protonation: 1600, 1557 (quasi-disappeared), 1502, 1454, 1417cm^{-1} and the band at 1634 cm^{-1} was appeared, indicating that pyridine rings have been successfully protonated (for a typical example see Figures 3B and B'). Similar spectral changes have been observed previously in protonation of P4VP [37]. It is noteworthy that thermogravimetric curves also show clear modifications between the pristine and protonated P4VP forms (see Figure 3C for a typical example).

Next, the hydrodynamic diameters (D$_h$) were determined for each particle (Figure 3A). Unfortunately, the direct comparison of pristine and protonated particles cannot be made since this D$_h$ value is directly influenced by the solvent used for dispersed the particles. For instance, the D$_h$ values of the pristine particles were of about 450 nm in water, 300 nm in ethanol/water solution (1:1 in volume), and 4 µm in heptane, whereas the [P4VPH][Cl] particles were close to 250 nm in water, 255 nm in ethanol/water solution (1:1 in volume), and 3 µm in heptane. In addition to the specific solvation, this behavior is related to the swelling capacity of the particles and their aggregation. Indeed, the crosslinking with DVB prevents the solubilization but not the solvation of P4VP chains. Thus, the reticulated particles can be swelled and aggregation can occur depending on the solvents used (see below and Figure 1). Consequently, the particle size is overestimated by DLS.

To better understand the structural morphology of P4VP and [P4VPH][Cl] particles, including their sizes, dry scanning and transmission electron microscopy (SEM and TEM) images were performed (Figure 4). As shown, the geometrical shape of particles is clearly affected by the protonation. Indeed, the morphology of the protonated P4VP beads is rather polydispersed and have a spherical shape with a mean diameter (D$_{SEM}$) of 147 ± 29 nm, regardless of the particles acidity. In contrast, the pristine P4VP particles are more monodispersed and have an ellipsoidal shape with major and minor diameters of 138 ± 11 and 60 ± 12 nm, respectively (the aspect ratio is about 2.3). In addition, the microstructures, observed by TEM, are also affected by the protonation. Indeed, the

protonated P4VP particles have a sponge-like amorphous morphology whereas the pristine ones exhibit a "faceted" structure due to the presence of crystalline or pseudo- crystalline domains (see Figure 4B). This observation can be related to the π-π stacking interactions between the aromatic rings of P4VP leading to well-ordered regions. In contrast, the electrostatic repulsions between pyridinium rings lead to a more amorphous porous structure (*i.e.* microgel texture).
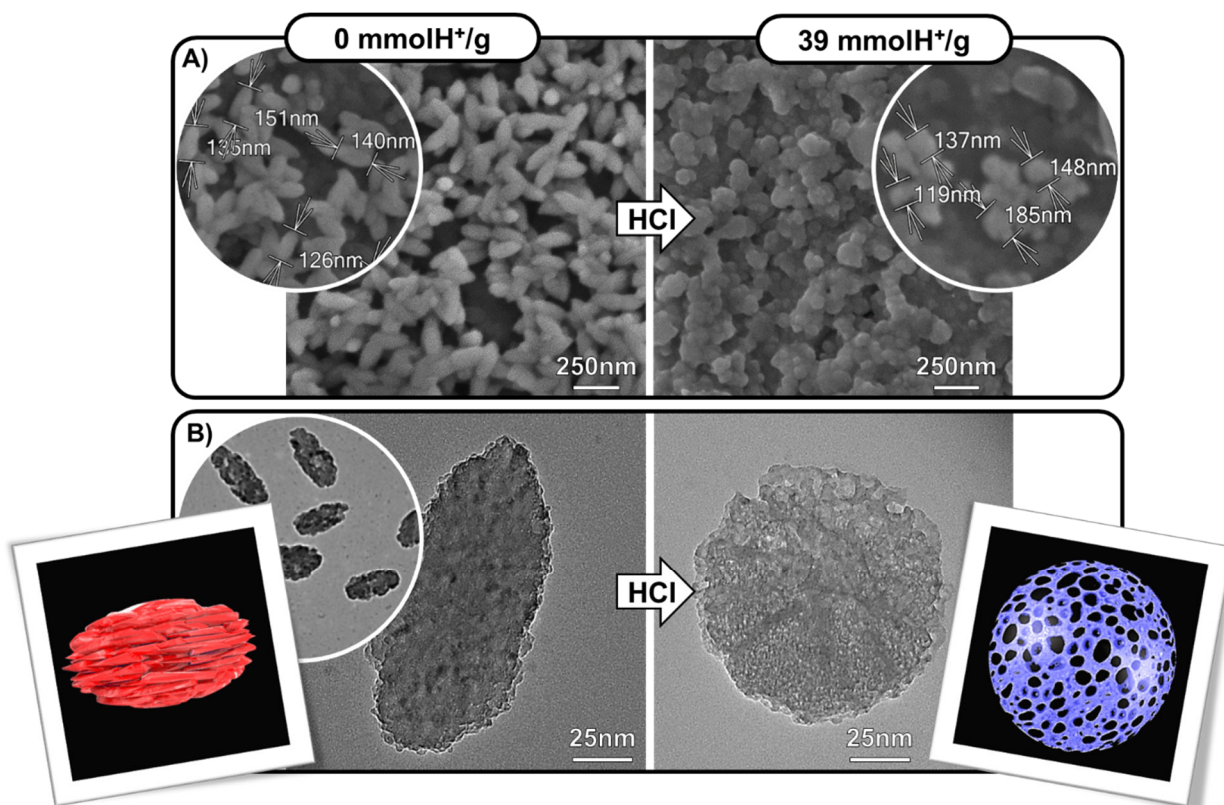

Figure 4. Typical SEM (**A**) and TEM (**B**) images showing the effect of protonation of P4VP particles observed after the evaporation of water by air-drying (see experimental section). The insets show the interpretation of TEM images.

In order to compare the protonated and neutral forms, the mean equivalent diameter of the ellipsoidal shaped P4VP particles (D'$_{SEM}$, taken as the diameter of a sphere of equivalent volume to that of non-spherical particles) is calculated using the following relation [38]:

$$D'_{SEM} = 1.55 \times A^{0.625}/P^{0.25} \qquad (1)$$

where A is the area and P is the perimeter of each particle obtained from the SEM images using Image J software (NIH, USA). The D'$_{SEM}$ of the native P4VP particles is about 88 ± 13 nm. The observed

shape transition is consistent with an increase in the repulsive interactions due to the large fraction of pyridinium residues present after acid treatment. Indeed, linear [P4VPH][Cl] are known to have an open morphology compared to neutral linear P4VP in order to minimize electrostatic repulsions [39]. Consequently, the transition from ellipsoidal to spherical shape is attributed in part to changes driven by repulsion of positively charged pyridine residues since a totally open polymer morphology is prohibited due to its reticulated nature. Moreover, as the increase in size between P4VP and [P4VPH][Cl] particles is very important (88 ± 13 *vs.* 147 ± 29 nm, respectively), we can hypothesize that the water molecules, strongly interact with the pyridinium groups, screening the electrostatic repulsions and promoting the particle shape change. In this case, these water molecules directly participate in the structural organization of [P4VPH][Cl] particles. This assumption is consistent with the thermogravimetric curves of P4VP and [P4VPH][Cl] particles (see two typical examples in Figure 3C). Indeed, the weight loss of P4VP and [P4VPH][Cl] particles increased gradually up to 150 °C due to the loss of water molecules (external hydration, 8 and 2% for [P4VPH][Cl] and P4VP particles, respectively). From 250 to about 450 °C, P4VP and [P4VPH][Cl] particles show a sharper weight loss, corresponding to the materials degradation (delayed for the pristine particles). However, it is noteworthy that [P4VPH][Cl] particles show an additional well-defined loss (mass change about 15% between 150 and 250 °C), assigned to an elimination of internal water molecules located in the spaces created by the repulsions between the charged pyridine residues. This observation supports the presence of interstitial and structural water molecules inside the [P4VPH][Cl] particles which prevents the formation of hollow ellipsoidal ones and their collapse. Consequently, the repulsions of positively charged pyridine residues, associated with the crosslinking with DVB and to the interstitial and structural water molecules, promote swelling of the P4VP ellipsoid to spherical shape upon acidification.

As the protonation changes the "hydrophobicity" of P4VP particles, the solid/liquid contact angles (θ) have been measured after a liquid is spread onto a solid substrate (*i.e.* compressed particles). Classically, θ gives an excellent indication of the hydrophobicity of particles. Indeed, if the testing

solvent is water, we have "hydrophilic" and "hydrophobic" particles for $\theta < 90°$ and $\theta > 90°$, respectively. The opposite holds for organic solvents (*e.g. n*-heptane). However, θ are not easily measurable with water and heptane due to their penetration in the internal structure of particles, thus confirming the swelling capacity of the particles previously mentioned. In order to overcome this problem, θ has been determined with more viscous solvents such as glycerol and paraffin oil ("hydrophilic" and "hydrophobic" solvents, see Figure 5). As expected the pristine P4VP is more "hydrophobic" ($112 \pm 1°$ and $40 \pm 2°$ for glycerol and paraffin oil, respectively) than the protonated ones. Moreover, the "hydrophilicity" increases with the protonation degree (see Figure 5).
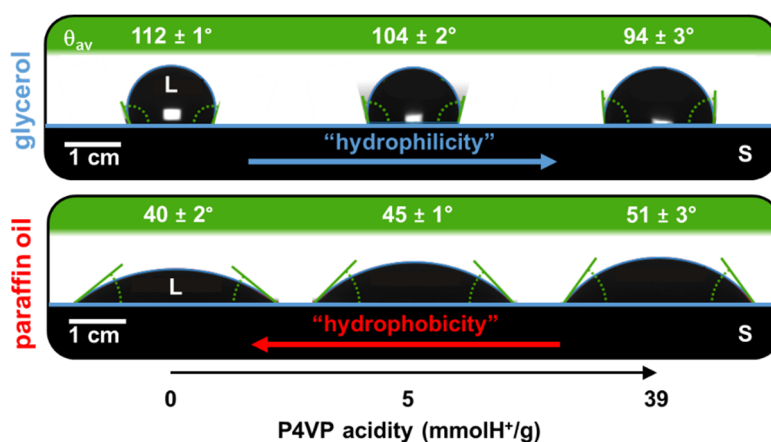

Figure 5. Typical photographs of glycerol or paraffin oil droplets (L) deposited on a compressed P4VP particles (S) as a function of protonation and average S/L contact angles (θ_{av}) after at least three measures.

Next, the ζ-potential and the conductivity of the P4VP particles, after isolation and redispersion in deionized water, were determined as a function of P4VP acidity (Figure 6). It is noteworthy that the stability of each P4VP dispersion was also evaluated using static multiple light scattering (SLMS) experiments by scanning over 1h the sample from the bottom to the top both in transmission and backscattering mode (both affected by particle size and volume concentration of the dispersion). According to the variation of light intensities over time, stability index (SI) can be calculated using the following relation:

$$SI = \sum_i \frac{\sum_h |scan_i(h) - scan_{i-1}(h)|}{H} \qquad (2)$$

where scan$_i$(h) and scan$_{i-1}$(h) are the scans of ith and i-1th time at a given height (h), and H is the total sample height. In this study, the SI values, recorded after 10 min, were also reported in Figure 6.
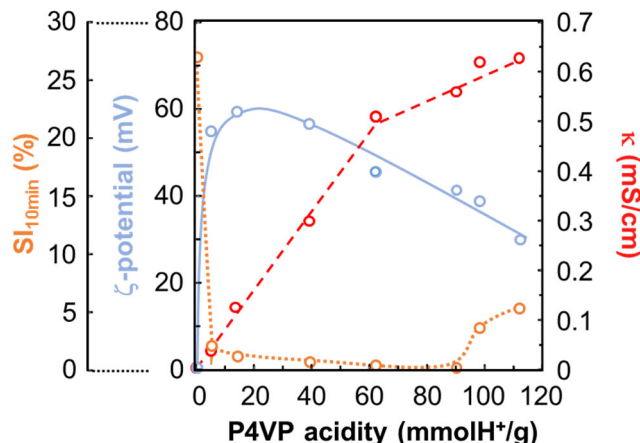

Figure 6. Conductivity (κ, S.D. ± 2%), ζ-potential (S.D. ±10 %) and stability index after 10 min (SI$_{10min}$) of aqueous dispersions plotted against the acidity of P4VP particles (0.05 wt.% in deionized water, S.D. ± 6%). The red dashed line was calculated using Eqs. 4 (optimized values: $\alpha^+ = 0.2\%$, $\alpha_1^- = 20\%$, and $\alpha_2^- = 6\%$).

As expected, the ζ-potential of all [P4VPH][Cl] was positive (from +60 to +30 mV) but surprisingly, it was decreased with increasing acidity. This reduction can be explained by an increase in the number of chloride ions adsorbed on the particles. This assumption is in agreement with conductivity results. Indeed, the conductivity increases with the increase of P4VP acidity with a certain slope. But at a critical [P4VPH][Cl] acidity ($C_C = 62$ mmolH$^+$/g), the slope changes. From a general point of view, the conductivity of [P4VPH][Cl] suspensions can be expressed as the sum of contributions of charged component as:

$$\kappa = \sum_i C_i \Lambda_i \qquad (3)$$

where C_i and Λ_i are the concentration and the specific conductivity of the ith component (with i = [P4VPH][Cl] particles or free HCl coming from the particles dissociation). As the [P4VPH][Cl] particles are much larger than the free HCl, it can be assumed that the charged particles do not contribute to the conductivity. As a slope change is observed at the breaking point, we can suppose that the free concentration of H$^+$ and Cl$^-$ varies below and above the critical [P4VPH][Cl] acidity. By

14

taking all these considerations into account, a model for fitting the conductivity curve can be expressed by the following set of equations:

$$\kappa = \begin{cases} \alpha^+\lambda^+C^+ + \alpha_1^-\lambda^-C^-, & C^- \leq C_C^- \\ \alpha^+\lambda^+C^+ + \alpha_1^-\lambda^-C_C^- + \alpha_2^-\lambda^-(C^--C_C^-), & C^- > C_C^- \end{cases} \quad (4)$$

where α^+, α_1^-, and α_2^- are the dissociation degrees of H^+, and Cl^- below and above C_C, respectively, λ^+ and λ^- are the limiting molar ionic conductivities of H^+ and Cl^- (349.8 and 76.3 mS/cm/M, respectively) [40], C^+ and C^- are the total concentrations of H^+ and Cl^- (assuming a complete ionization of [P4VPH][Cl] particles, note that $C^+ = C^-$), and C_C^- is the total chloride concentration at the critical [P4VPH][Cl] acidity (3.1 mM for $C_C = 62$ mmolH$^+$/g). For each [P4VPH][Cl] particle (varying only by its acidity), the experimental α^+ value can easily be estimated as the ratio between the [H$^+$] released by particles dispersed in water (measured using a pH-meter) and the C^+. The obtained α^+ value is found to be totally independent of the P4VP acidities (0.2 ± 0.1 %). With this result in hand, it is possible to fit the experimental conductivity data below and above C_C with the appropriate constants (*i.e.* α_1^- and α_2^-) using Eqs. 4. The conductivity curve can be well fitted by using the model and the α_1^- and α_2^- constants can be estimated at 20 and 6%, respectively ($R^2 = 0.9975$, see Figure 6). Therefore the conductivity and ζ-potential measurements are in good agreement confirming that the breaking point, observed at C_C, is due to the binding of chlorides to the particles when the charge density increases on the particles (*i.e.* for P4VP acidity > 62 mmolH$^+$/g). Obviously, the accumulation of chlorides onto the surface of the most acidic particles leads to the destabilization of the sample by sedimentation (see the SI values, Figure 6). Therefore, we can predict that the particles with the highest ζ-potential values (*i.e.* for P4VP acidity ≤ 90 mmolH$^+$/g) will show higher electrostatic repulsions preventing the particles aggregation and leading to stable Pickering emulsions.

Before studying in detail the Pickering emulsions stabilized by protonated P4VP particles, we explored the effects of various organic solvents (*i.e.* oil phases) on the Pickering stabilization. Indeed, the nature of the oil directly affecting the wetting of the particles and the emulsion stabilization, the

choice of the oil is therefore crucial. Obviously, the selection criterion of these oils was their complete or high immiscibility with the aqueous phase. The investigated oils include hydrocarbons (*e.g. n*-heptane and toluene), halogenated hydrocarbons (*e.g.* dichloromethane, DCM) and hydrogen bond acceptor solvents (*e.g.* cyclopentyl methyl ether, CPME, and 2-methyl tetrahydrofuran, MTHF). The oil ability to provide Pickering emulsions was thus correlated with the Kamlet and Taft parameters used as descriptors of the solvent properties (H-bond donor ability, α, H-bond acceptor ability, β, and polarity, π^*, see Figure 7). All other parameters were kept constant such as the particle concentration (1 wt.% of [P4VPH][Cl] at 14 mmolH$^+$/g), the water/oil ratio (49.5 wt.% each) and the emulsification process (11,500 rpm, 60 s, 25 °C). Regardless of the solvent used, pristine P4VP (used as control experiments) never succeeds in stabilizing Pickering emulsions. As shown in Figure 7, only hydrocarbons and halogenated hydrocarbons (*n*-heptane, toluene and DCM) made it possible to obtain Pickering emulsions with an emulsion volume fraction of 100% (v/v) just after emulsification. In contrast, CPME and MTHF provided only partial emulsions. Therefore, the emulsification ability of oils increases in the order CPME ≈ MTHF ≪ *n*-heptane ≈ toluene ≈ DCM , which is compatible with a modulation of the local environment. Indeed, the oil polarity induces a change in the emulsification ability due to the intermediate wettability of the [P4VPH][Cl], which has hydrophilic and hydrophobic domains (*i.e.* charged or uncharged pyridine units, respectively). As the stabilizing ability of [P4VPH][Cl] is improved with non-polar oils than more polar oils (*i.e.* H-bond acceptor solvents), we propose that this dependence is due to solvation and/or porosity of the particles that allows the adsorption of non-polar solvents onto the particle surface or inside (see above). This phenomenon can be related to the hydrophobic interactions between the non-polar molecules and the [P4VPH][Cl] hydrophobic domains (*i.e.* van der Waals forces). It is noteworthy that complementary interactions such as π-π stacking take place between the aromatic rings of [P4VPH][Cl] particles and toluene molecules. In contrast, for H-bond acceptor solvents, interactions through electrostatic forces can be expected between the cationic pyridinium group and the oxygen atoms of the solvents. This

solvation leads to the interfacial charge screening of the [P4VPH][Cl] making the particles too hydrophobic to stabilize Pickering emulsions as in the case of pristine P4VP.
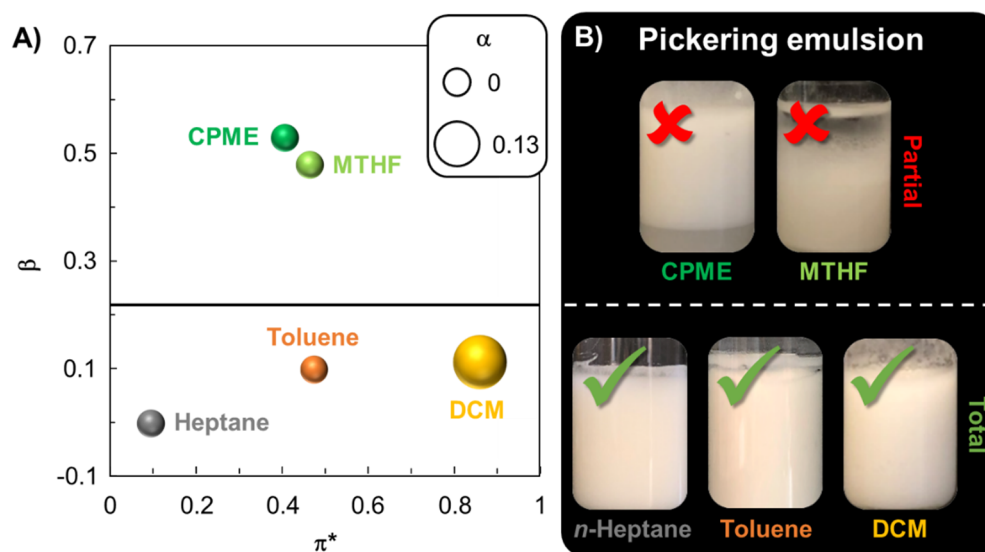

Figure 7. (**A**) Kamlet-Taft parameters (H-bond donor ability, α, H-bond acceptor ability, β, and polarity, π^*, values taken from ref. 41) of investigated oils (CPME = cyclopentyl methyl ether, MTHF = 2-methyl tetrahydrofuran, DCM = dichloromethane) and (**B**) photographs of water/oil Pickering emulsions stabilized by [P4VPH][Cl] particles at 14 mmolH$^+$/g (49.5/49.5/1 wt.%, 11,500 rpm, 60 s, 25 °C).

Based on these observations, *n*-heptane-based Pickering emulsions have served as model systems in the following discussion. Nevertheless, the observations, described below, can be extended to all hydrocarbons and halogenated hydrocarbons. In spite of everything, it is noteworthy that a slow phase separation is observed with time but without total phase separation for emulsions stabilized by non-polar oils including *n*-heptane. Consequently, the heptane-based system was optimized to provide stable emulsions. The general composition of the stable systems is: 5 wt.% of [P4VPH][Cl] particles supplemented with water and *n*-heptane (47.5 wt.% each). The emulsification was performed over 60 s at 11,500 rpm and 25 °C. In more detail, for pristine P4VP, used as a control experiment, a coarse heterogeneous whitish phase, composed of aggregated solvated particles, was observed at mid-height of the tube with upper heptane and lower aqueous phase. This observation confirms that P4VP particles are too hydrophobic to stabilize Pickering emulsions. Similar behavior is observed for

[P4VPH][Cl] at 5 mmolH⁺/g due to an unfavorable amphiphilic balance. Indeed, despite a slight increase in charge density by protonation, the latter remained too hydrophobic to stabilize Pickering emulsions. As expected, for [P4VPH][Cl] particles with acidity > 90 mmolH⁺/g, we observed systems composed of three phases: limpid heptane, water in which some [P4VPH][Cl] particles were dispersed, and a large excess of particles at the sample bottom. Again, a disadvantageous amphiphilic balance is observed (too hydrophilic this time). In contrast, the acidic particles between 14 and 90 mmolH⁺/g provided homogeneous whitish emulsions with an aqueous external phase as evidenced by the measurement of electrical conductivity. The emulsion volume fractions, the mean droplet diameters and some typical photomicrographs of heptane-in-water emulsions are shown in Figure 8.
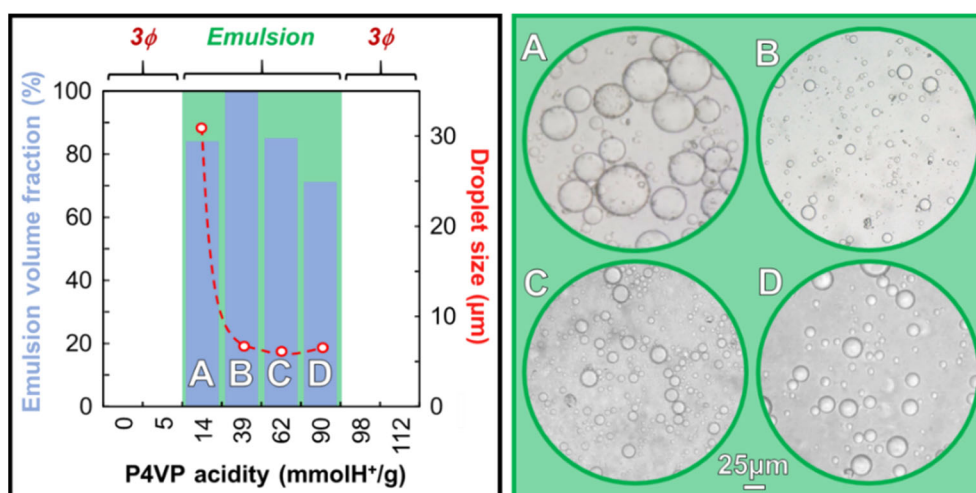

Figure 8. Emulsion volume fractions (S.D. ± 2%), mean droplet diameters (S.D. ± 10%) and typical photomicrographs of heptane-in-water Pickering emulsions stabilized by [P4VPH][Cl] or pristine P4VP particles (water/heptane/particles 47.5/47.5/5 wt.%, 11,500 rpm, 60 s, 25 °C).

As it can be seen, the acidic particles of 39 mmolH⁺/g were more effective in emulsifying heptane in water than the three other ones (emulsion volume fraction = 100% and oil droplets = 7 ± 1 μm). This observation can be directly related to the optimal amphiphilic balance and to the ζ-potential acquired in water (+57 ± 6 mV, see above). Indeed, this high ζ-potential allows a higher electrostatic repulsions leading to the inhibition of the coalescence phenomenon. This assertion is corroborated with the emulsion stability, since no destabilization was observed when increasing the temperature at 60 °C for 3 hours.

The destabilization mechanisms of the emulsions can be identified by SMLS since the backscattered light (ΔBS) is related to droplet migration, droplet size and phases thickness (Figure 9A) [42].
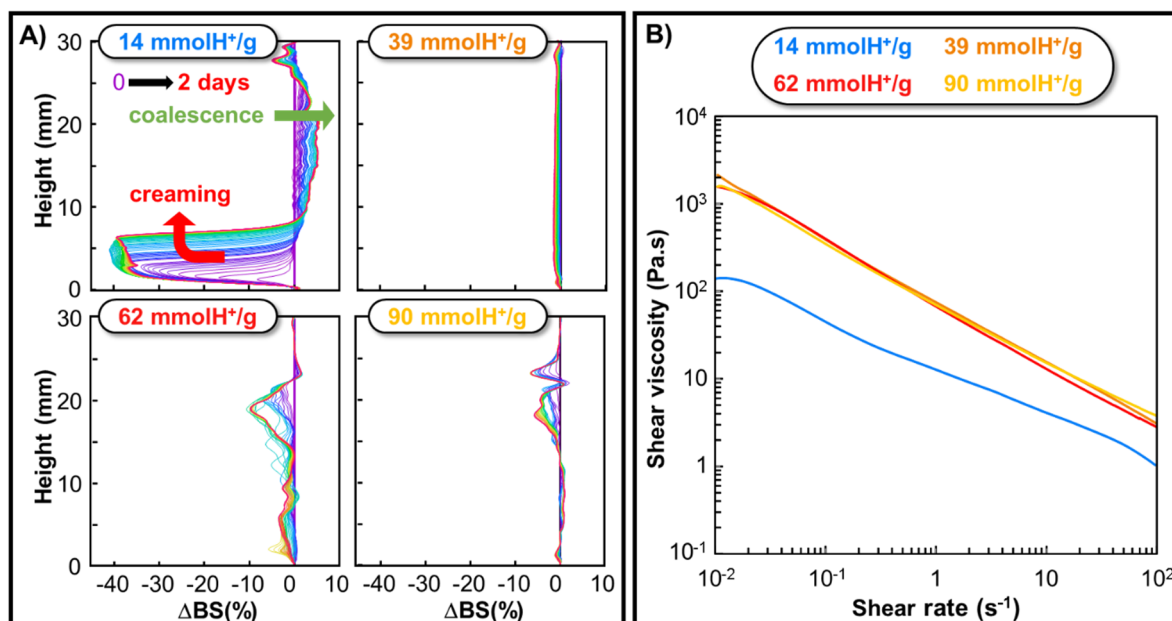

Figure 9. Backscattering (ΔBS) versus sample height and time at 25 °C (**A**) and shear viscosity as a function of shear rate (**B**) for heptane-in-water emulsions stabilized by [P4VPH][Cl] particles of different acidity (water/heptane/particles 47.5/47.5/5 wt.%, 11,500 rpm, 60 s, 25 °C).

For the acidic particles of 14 mmolH$^+$/g, a creaming was detected as the ΔBS over time decreases at the sample's bottom whereas the increase of ΔBS at the mid-height indicated a coalescence process (*i.e.* droplet size variation). For the three other [P4VPH][Cl] particles, a slight droplet size variation due to coalescence was also observed. As the sample with the smallest ΔBS variation over time is the most stable: the acidic particles of 39 mmolH$^+$/g were qualitatively more stable. However, the coalescence process cannot be considered as a true instability since it is limited. Indeed, this process is conventionally observed when the surface of the droplets covered by the particles is partial leading to coalescence until a compact monolayer is obtained. For instance, the emulsion stabilized by the acidic particles of 39 mmolH$^+$/g exhibits a long-term stability since the volume fraction was still 100% and that the mean droplet size did not change appreciably after one year at room temperature. Moreover, even centrifugation (5,000 rpm for 20 min) failed to destabilize this emulsion. In contrast,

for the acidic particles of 14 mmolH$^+$/g, the creaming is undesirable because it causes difficulties to storage and handling. In addition, this variation in stability can also be attributed to the macroscopic texture of the emulsions which are in the form extremely thick pasty systems with the exception of that stabilized by the acid particles of 14 mmolH$^+$/g which give a creamy texture due to a smaller droplet size (31 ± 3 *vs.* 7 ± 1 μm, see Figure 8). These observations are perfectly corroborated with the viscosity of the Pickering emulsions (Figure 9B). A clear divergence between the emulsion stabilized by the acidic particles of 14 mmolH$^+$/g and the other three is observed. Indeed, the shear viscosity of the emulsion stabilized by the acidic particles of 39 mmolH$^+$/g is on average 12-fold higher than that stabilized by the acid particles of 14 mmolH$^+$/g. This evolution seems to be dependent on the droplet size of the emulsion: high-emulsion viscosity is obtained for very fine droplet size (compare Figures 8 and 9B). However, the emulsions are highly viscous under storage conditions, but exhibit low viscosity under shear rate: their viscosity is inferior to 4 Pa.s at 100 s^{-1}.

In order to investigate the packing and ordering of the particles at the oil-water interface, SEM experiments were performed. The heptane-in-water emulsion stabilized by [P4VPH][Cl] particles at 39 mmolH$^+$/g was deposited onto a carbon conductive adhesive tape stuck on a stub. The "ghost" emulsion could be observed using a conventional SEM after evaporation of water and heptane-core by air-drying and chromium coating [43]. SEM images of the "ghost" emulsion are shown in Figure 10. Interestingly, "ghost" droplets are covered by a densely packed particle layer. However, the droplet sizes were seemed to be higher than observed ones by optical microscopy (around 15-20 vs. 7 ± 1 μm) probably due to an artefact due to the sample preparation prior to SEM imaging. Indeed, the evaporation of heptane-core by air-drying could result in a greater or lesser extension of droplet sizes in accord with the vaporization rate. For instance, if the vaporization is fast (vacuum treatment), the emulsions structures are totally collapsed. In contrast, with an appropriate evaporation, we can observe intact droplets (Figure 10C). As it can be seen, a careful look at the droplet surface reveals the presence of very large [P4VPH][Cl] particles whose shape and size are clearly different from those observed after a simple aqueous dispersion (around 1-5 μm *vs.* 147 ± 29 nm). Moreover, the

particles are very densely packed around the droplets leading to a complex network after solvent vaporization. However, this particles packing is impossible without very strong attractive forces between the particles since the particles are positively charged (+57 ± 6 mV, see above).

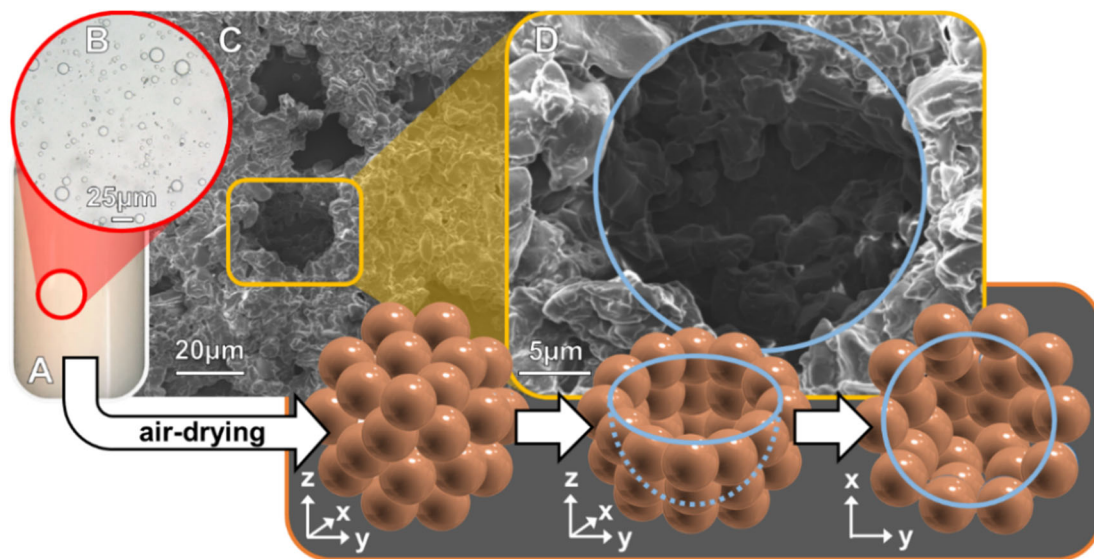**Figure 10.** Macroscopic view (**A**), photomicrograph (**B**) and electron micrograph, observed by SEM after vaporization of water and heptane-core by air-drying, (**C** and **D**) of heptane-in-water emulsion stabilized by [P4VPH][Cl] particles (water/heptane/particles 47.5/47.5/5 wt.%, 11,500 rpm, 60 s, 25 °C). The inset shows the interpretation of SEM images.

Therefore, the question is what is the origin of this attraction? A plausible explanation is that the dense interfacial packing is due to the penetration of heptane inside the particles leading to their swelling and to their aggregation (bridging mechanism using heptane molecules, see Figure 1). Consequently, the particles are fused or coagulated with a loss of their initial spherical shape and an increase in their apparent size. This assertion is confirmed by the measurement of D_h of [P4VPH][Cl] particles in heptane which provides an apparent size of 3 µm (see above). The bridging mechanism compensates for the long-ranged coulombic repulsion caused by the charges at the particle surface. It is noteworthy that the complex network structure can be due to the capillary forces that are probably particularly pronounced with the rough fused particles formed. Obviously, this network is involved in the very good stability as well as in the high viscosity of the emulsion stabilized by [P4VPH][Cl] particles at 39 mmolH$^+$/g (see above).

Next, the destabilization of the Pickering emulsion stabilized by [P4VPH][Cl] particles were investigated due to the potential applications of this system in organic synthesis for example. Indeed, the properties of the Pickering emulsion stabilized by [P4VPH][Cl] particles at 39 mmolH$^+$/g (*i.e.* large interface area with unprecedented resistance against centrifugation and high temperatures) make such a system of particular interest for biphasic reactions in which the stabilizing particles would act as reagent proton, scavenger, and/or catalyst. Our physicochemical results support that the destabilization could easily be obtained by extreme pH changes since neutral and very acid (> 90 mmolH$^+$/g) particles are unable to stabilize Pickering emulsions (see Figure 8). In addition, ionic strength variations also appear to be able to destabilize the emulsions since the accumulation of chlorides onto the surface of the most acidic particles leads to the phase separation by sedimentation (see Figure 6). For this purpose, the effect of adding aqueous solutions of HCl, NaOH or NaCl on the Pickering emulsion stabilized by [P4VPH][Cl] particles at 39 mmolH$^+$/g is reported in Figure 11A (room temperature without stirring).
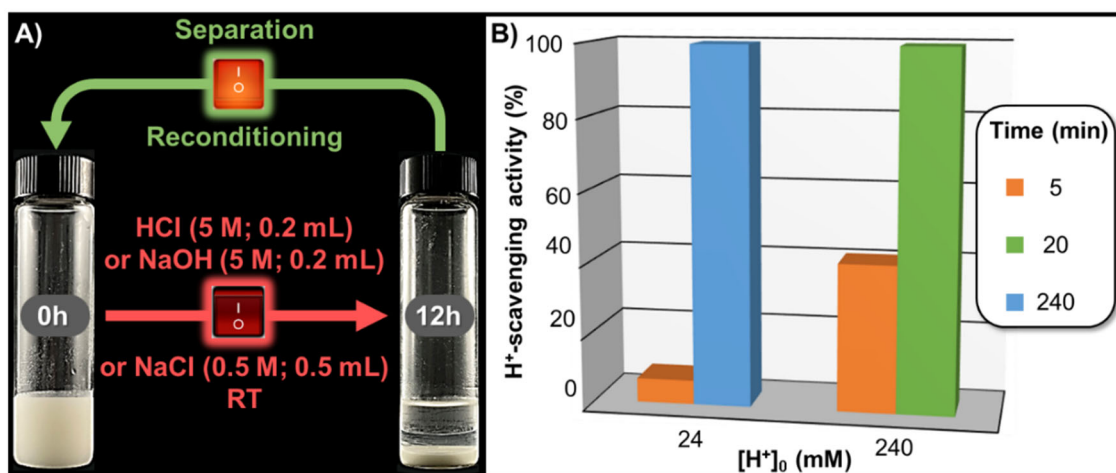

Figure 11. Destabilization by pH and ionic strength changes (**A**), and H$^+$-scavenging activity as a function of time and initial [H$^+$]$_0$ concentration in aqueous phase, (**B**) of heptane-in-water emulsions (47.5 wt.% each) stabilized by [P4VPH][Cl] particles at 39 mmolH$^+$/g (5 wt.%).

As expected, the phase separations were obtained after 12 hours. On the other hand, it should be noted that addition of neat water to the emulsions does not destabilize them (control experiment). In this case, the emulsions are simply diluted. The particles can be washed thoroughly with demineralized

water to remove the electrolytes (until neutral pH) and then dried before reconditioning them (see above) in order to provide new emulsions. It is noteworthy that the size of droplet is slightly increased after recycling (11 ± 1 *vs*. 7 ± 1 µm) due to the low loss of particles incurred during the recovery.

Finally, since P4VP is widely used as a scavenger, we have evaluated the proton-scavenging activity of the Pickering emulsion containing 5 wt.% of [P4VPH][Cl] at 39 mmol of H^+ per gram. From a theoretical point of view, 100g of such an emulsion are able to fix a maximum value of 365 mmol of H^+ (*i.e.* five times the difference between the maximum capacity that can be obtained and that of the particle used, each expressed in the form of acid density; mmol H^+/g) corresponding to 7.68 M of HCl in the aqueous phase. As this value is very far from the reaction media commonly used, we therefore tested more realistic concentrations. In addition, emulsions no longer exist at this concentration (see above). In respect with this, two Pickering emulsions were prepared using 47.5 wt.% of aqueous HCl solution ($[H^+]_0 = 24$ or 240 mM) supplemented with 47.5% of heptane and 5% of particles at 39 mmolH^+/g. After emulsification over 60s at 11,500 rpm, the systems were stirred at 200 rpm at 25 °C. After a given time, the free H^+ concentration $[H^+]_t$ was measured using a pH-meter and the H^+-scavenging activity was calculated as the ratio between the scavenged H^+ concentration, $[H^+]_0$-$[H^+]_t$, and $[H^+]_0$. The H^+-scavenging activity varies as a function of initial HCl concentration in aqueous phase and as a function of time (see Figure 11B). For instance, after 5 min of contact, the H^+-scavenging activities were of 7 and 41% for 24 and 240 mM of $[H^+]_0$. On the other hand, the time needed to obtain an activity >99% is of 240 and 20 min for 24 and 240 mM of $[H^+]_0$. These both observations reflect that the rate-determining step is the H^+ concentration and its diffusion. Moreover, it is noteworthy that the phase separation was progressively achieved during the contact time. All these findings show that the [P4VPH][Cl] particles can be used as a route to easily manage the phase separation in Pickering emulsions using "on-off" switches based on pH and ionic strength with potential practical applications in synthesis [44].

4. Conclusion

In this study, we developed oil-in-water Pickering emulsions stabilized by partially protonated crosslinked poly(4-vinylpyridine) particles (P4VP). The charge density of particles could be finely adjusted from 0 to 112 mmolH$^+$/g. The physicochemical data revealed that the protonated P4VP particles with 39 mmolH$^+$/g were more effective in emulsifying heptane in water than pristine or higher protonated ones. The obtained emulsion exhibited excellent stability against centrifugation and temperature (up to 5,000 rpm and 60 °C). Nevertheless, the phase separation can be easily controlled using "on-off" switches based on pH and ionic strength, facilitating at the same time the particle recovery. In contrast to the previous works, which used synthesized P4VP-based microgel particles, the raw material (*i.e.* crosslinked P4VP) is inexpensive, commercially available and can be used without chemical transformation (*e.g.* (co)polymerization, cross-linking, grafting, *etc.*) to lead to very simple and cheap responsive Pickering emulsion systems [22, 28-33]. In addition, our results support that the degree of control arises from the swelling capacity of crosslinked P4VP particles, confirming the commonly accepted mechanism [22-24]. Contrary to the literature data on responsive Pickering emulsions [28-33] and in respect with the Leonardo da Vinci quote ("*simplicity is the ultimate sophistication*"), our system provides a facile route to construct "on-off" switches by simply using P4VP cross-linked particles which possess changeable structures based on electrostatic repulsions. Moreover, the flexibility of the proposed system could be used to load various catalytic metal cations (such as Cu, Ru, Au, Zn, *etc.*) since the P4VP polymers are known to complex them thanks to the pyridine units [45-47]. As such responsive emulsions are very attractive to perform chemical transformations in biphasic media, in which the P4VP particles would act as a reagent, scavenger, catalyst, and/or ligand of metal ions, work is underway in our group to develop practical applications with significant environmental and economic perspectives in organic synthesis.

CRediT authorship contribution statement

Grégory Douyère: Methodology, Investigation, Data curation, Writing - original draft. Loïc Leclercq: Conceptualization, Formal analysis, Visualization, Supervision, Writing - review & editing.

Véronique Nardello-Rataj: Conceptualization, Supervision, Funding acquisition, Project administration, Validation.

Declaration of competing interest

The authors declare that they have no known competing financial interests or personal relationships that could have appeared to influence the work reported in this paper.

Acknowledgements

References

[1]   T. Zhang, J. Xu, J. Chen, Z. Wang, X. Wang, J. Zhong, Protein nanoparticles for Pickering emulsions: A comprehensive review on their shapes, preparation methods, and modification methods. Trends Food Sci. Technol. 113 (2021) 26-41. DOI: 10.1016/j.tifs.2021.04.054.

[2]   Abdullah, J. Weiss, T. Ahmad, C. Zhang, H. Zhang, A review of recent progress on high internal-phase Pickering emulsions in food science, Trends Food Sci. Technol. 106 (2020) 91-103. DOI: 10.1016/j.tifs.2020.10.016.

[3]   C. Albert, M. Beladjine, N. Tsapis, E. Fattal, F. Agnely, N. Huang, Pickering emulsions: Preparation processes, key parameters governing their properties and potential for pharmaceutical applications, J. Control. Release 309 (2019) 302-332. DOI: 10.1016/j.jconrel.2019.07.003.

[4]   J. Tang, P.J. Quinlan, K.C. Tam, Stimuli-responsive Pickering emulsions: recent advances and potential applications, Soft Matter 11 (2015) 3512-3529. DOI: 10.1039/c5sm00247h.

[5] L. Leclercq, J. Tessier, V. Nardello-Rataj, A.-R. Schmitzer, Highly active, entirely biobased antimicrobial Pickering emulsions, ChemMedChem 16 (2021) 2223-2230. DOI: 10.1002/cmdc.202100030.

[6] Y. Yang, Z. Fang, X. Chen, W. Zhang, Y. Xie, Y. Chen, Z. Liu, W. Yuan, An Overview of Pickering Emulsions: Solid-Particle Materials, Classification, Morphology, and Applications. Front. Pharmacol. 8 (2017) 287. DOI: 10.3389/fphar.2017.00287.

[7] Y. He, F. Wu, X. Sun, R. Li, Y. Guo, C. Li, L.u. Zhang, F. Xing, W. Wang, J. Gao, Factors that affect Pickering emulsions stabilized by graphene oxide, ACS Appl. Mater. Interfaces 5 (11) (2013), 4843-4855. DOI: 10.1021/am400582n.

[8] B. Yang, L. Leclercq, V. Schmitt, M. Pera-Titus, V. Nardello-Rataj, Colloidal tectonics for tamdem sygnegistic Pickering interfacial catalysis: oxidative cleavage of cyclohexene oxide into adipic acid, Chem. Sci. 10 (2) (2019) 501-507. DOI: 10.1039/c8sc03345e.

[9] J. Luo, M. Zeng, B. Peng, Y. Tang, L. Zhang, P. Wang, L. He, D. Huang, L. Wang, X. Wang, M. Chen, S. Lei, P. Lin, Y. Chen, Z. Cheng, Electrostatic-driven dynamic jamming of 2D nanoparticles at interfaces for controlled molecular diffusion, Angew. Chem. Int. Ed. 57 (36) (2018), 11752-11757. DOI: 10.1002/anie.201807372.

[10] J.B. Mougel, P. Bertoncini, B. Cathala, O. Chauvet, I. Caprona, Macroporous hybrid Pickering foams based on carbon nanotubes and cellulose nanocrystals, J. Colloid Interface Sci. 544 (2019) 78-87. DOI: 10.1016/j.jcis.2019.01.127.

[11] B.V. Farias, D. Brown, A. Hearn, N. Nunn, O. Shenderov, S.A. Khana, Nanodiamond-stabilized Pickering emulsions: Microstructure and rheology, J. Colloid Interface Sci. 580 (2020) 180-191. DOI: 10.1016/j.jcis.2020.07.030.

[12] G. Sun, X. Liu, D. J. McClements, S. Liu, B. Li, Y. Li, Chitin nanofibers improve the stability and functional performance of Pickering emulsions formed from colloidal zein, J. Colloid Interface Sci. 589 (2021) 388-400. DOI: 10.1016/j.jcis.2021.01.017.

[13] Q. Jiang, S. Li, L. Du, Y. Liu, Z. Meng, Soft κ-carrageenan microgels stabilized Pickering emulsion gels: Compact interfacial layer construction and particle-dominated emulsion gelation, J. Colloid Interface Sci. 602 (2021) 822-833. DOI: 10.1016/j.jcis.2021.06.070.

[14] L. Leclercq, J. Tessier, G. Douyère, V. Nardello-Rataj, A.R- Schmitzer, Phytochemical- and cyclodextrin-based Pickering emulsions: natural potentiators of antibacterial, antifungal, and antibiofilm activity, Langmuir 36 (16) (2020) 4317-4323. DOI: 10.1021/acs.langmuir.0c00314.

[15] L. Leclercq, Get beyond limits: from colloidal tectonics concept to the engineering of eco-friendly catalytic systems, Front. Chem. 6 (2018) 168. DOI: 10.3389/fchem.2018.00168.

[16] H. Liu, C. Wang, S. Zou, Z. Wei, Z. Tong, Simple, reversible emulsion system switched by pH on the basis of chitosan without any hydrophobic modification, Langmuir 28 (30) (2012), 11017-11024. DOI: 10.1021/la3021113.

[17] Q. Mao, M. Li, S. Zhang, X. Zhang, G. He, W. Zhang, Chitosan-hydrophobic alginate nanocomposites stabilized pH-triggered Pickering emulsion for drug controlled-release, Int. J. Biol. Macromol. 162 (2020) 1888-1896. DOI: 10.1016/j.ijbiomac.2020.08.092.

[18] A. Schrade, K. Landfester, U. Ziener, Pickering-type stabilized nanoparticles by heterophase polymerization, Chem. Soc. Rev. 42 (16) (2013), 6823-6839. DOI: 10.1039/c3cs60100e.

[19] M. Pera-Titus, L. Leclercq, J.-M. Clacens, F. De Campo, V. Nardello-Rataj, Pickering interfacial catalysis for biphasic systems: from emulsion design to green reactions, Angew. Chem. Int. Ed. 54 (2015) 2006-2021. DOI: 10.1002/anie.201402069.

[20] H. Jiang, Y. Sheng, T. Ngai, Pickering emulsions: Versatility of colloidal particles and recent applications, Curr. Opin. Colloid Interface Sci. 49 (2020) 1-15. DOI: 10.1016/j.cocis.2020.04.010.

[21] E. Dickinson, Microgels: An alternative colloidal ingredient for stabilization of food emulsions, Trends Food Sci. Technol. 43 (2) (2015), 178-188. DOI: 10.1016/j.tifs.2015.02.006.

[22] B.P. Binks, R. Murakami, S.P. Armes, S. Fujii, Effects of pH and salt concentration on oil-in-water emulsions stabilized solely by nanocomposite microgel particles, Langmuir 22 (5) (2006) 2050-2057. DOI: 10.1021/la053017+.

[23] Z. Li, To Ngai, Microgel particles at the fluid-fluid interfaces, Nanoscale 5 (4) (2013) 1399-1410. DOI: 10.1039/c2nr33503d.

[24] M.-C. Tatry, P. Galanopoulo, L. Waldmann, V. Lapeyre, P. Garrigue, V. Schmitt, V. Ravaine, Pickering emulsions stabilized by thermoresponsive oligo(ethylene glycol)-based microgels: Effect of temperature-sensitivity on emulsion stability, J. Colloid Interface Sci. 589 (2021) 96-109. DOI: 10.1016/j.jcis.2020.12.082.

[25] B. Brugger, W. Richtering, Emulsions stabilized by stimuli-sensitive poly(n-isopropylacrylamide)-co-methacrylic acid polymers: microgels versus low molecular weight polymers, Langmuir 24 (15) (2008) 7769-7777. DOI: 10.1021/la800522h.

[26] S. Wiese, A.C. Spiess, W. Richtering, Microgel-stabilized smart emulsions for biocatalysis, Angew. Chem. Int. Ed. 52 (2) (2013) 576-579. DOI: 10.1002/anie.201206931.

[27] S. Dai, P. Ravi, K.C. Tam, pH-Responsive polymers: synthesis, properties and applications, Soft Matter 2008 4 (3) (2008) 435-449. DOI: 10.1039/b714741d.

[28] S. Fujii, E. S. Read, B. P. Binks, S. P. Armes, Stimulus-responsive emulsifiers based on nanocomposite microgel particles, Adv. Mater. 17 (8) (2005) 1014-1018. DOI: 10.1002/adma.200401641.

[29] Z. Fang, D. Yang, Y. Gao, H. Li, pH-responsible Pickering emulsion and its catalytic application for reaction at water–oil interface. Colloid Polym. Sci. 293 (2015) 1505-1513. DOI: 10.1007/s00396-015-3533-8.

[30] A.M. Atta, A.O. Ezzat, H. A. Al-Lohedan, A.M. Tawfeek, A.A. Alobaidi, Preparation of pH responsive polystyrene and polyvinyl pyridine nanospheres stabilized by mickering microgel emulsions, Nanomaterials 9(12) (2019) 1693. DOI: 10.3390/nano9121693.

[31] N. Sahiner, A.M. Atta, A.O. Yasar, H.A. Al-Lohedan, A.O. Ezzat, Surface activity of amphiphilic cationic pH-responsive poly(4-vinylpyridine) microgel at air/water interface, Colloids Surf. A Physicochem. Eng. Asp. 482 (2015) 647-655. DOI: 10.1016/j.colsurfa.2015.07.035.

[32] K. Kim, B. Vincent, pH and Temperature-sensitive behaviors of poly(4-vinyl pyridine-co-n-isopropyl acrylamide) microgels. Polym. J. 37 (2005) 565-570. DOI: 10.1295/polymj.37.565.

[33] T. Zeng, A. Deng, D. Yang, H. Li, C. Qi, Y. Gao, Triple-responsive Pickering emulsion stabilized by core cross-linked supramolecular polymer particles, Langmuir 35 (36) (2019) 11872-11880. DOI: 10.1021/acs.langmuir.9b02341.

[34] L. Leclercq, I. Suisse, G. Nowogrocki, F. Agbossou-Niedercorn, Halide-free highly-pure imidazolium triflate ionic liquids: Preparation and use in palladium-catalysed allylic alkylation, Green Chem. 9 (10) (2007) 1097-1103. DOI: 10.1039/b703096g.

[35] F. Espinola-Portilla, O. Serrano-Torres, G.F. Hurtado-López, U. Sierra, A. Varenne, F. d'Orlyé, L. Trapiella-Alfonso, S. Gutiérrez-Granados, G. Ramírez-García, Superparamagnetic iron oxide nanoparticles functionalized with a binary alkoxysilane array and poly(4-vinylpyridine) for magnetic targeting and pH-responsive release of doxorubicin, New J. Chem. 45 (7) (2021) 3600-3609. DOI: 10.1039/d0nj05227b.

[36] L. Franck-Lacaz, P. Sistat, P. Huguet, Determination of the pKa of poly (4-vinylpyridine)-based weak anion exchange membranes for the investigation of the side proton leakage, J. Membr. Sci. 326 (2) (2009) 650-658. DOI: 10.1016/j.memsci.2008.10.054.

[37] Y.D. Vorontsov, V.P. Panov, Vibrational spectra of protonated poly-4-vinylpyridine, Polym. Sci. USSR 18 (11) (1976) 2752-2759. DOI: 10.1016/0032-3950(76)90212-4.

[38] J. W. Heyt, M. J. Diaz, Equivalent Diameters of Rectangular and Oval Ducts, ASHRAE Trans. 81 (2) (1975) 221-232.

[39] Y. Zang, H. Zhu, H. Xue, Design of a novel "ON-OFF" switchable enzymatic biofuel cell based on pH-sensitive PS-b-P4VP diblock copolymer, Electrochim. Acta 259 (2018) 676-684. DOI: 10.1016/j.electacta.2017.11.023.

[40] P. Vanýsek, "Equivalent Conductivity of Electrolytes in Aqueous Solution" In *CRC Handbook of Chemistry and Physics*, 99th edition, J. R. Rumble (Ed.), CRC Press/Taylor & Francis: Boca Raton, FL, USA, 2018.

[41] A. Duereh, Y. Sato, R. Lee Smith, Jr., H. Inomata, Methodology for replacing dipolar aprotic solvents used in API processing with safe hydrogen-bond donor and acceptor solvent-pair mixtures, Org. Process Res. Dev. 21 (1) (2017) 114-124. DOI: 10.1021/acs.oprd.6b00401.

[42] L. Leclercq, V. Nardello-Rataj, Pickering emulsions based on cyclodextrins: A smart solution for antifungal azole derivatives topical delivery, Eur. J. Pharm. Sci. 82 (2016) 126-137. DOI: 10.1016/j.ejps.2015.11.017.

[43] L. Leclercq, J.-F. Dechézelles, G. Rauwel, V. Nardello-Rataj, In vitro study of versatile drug formulations based on α-cyclodextrin and polyethylene glycol using colloidal tectonics, J. Drug Deliv. Sci. Technol. 59 (2020) 101913. DOI: 10.1016/j.jddst.2020.101913.

[44] N.G. Khaligh, H.S. Abbo, M.R. Johan, S.J.J. Titinchi, Poly(vinyl pyridine)s: A versatile polymer in catalysis, Curr. Org. Chem. 23 (4) (2019) 439-479. DOI: 10.2174/1385272823666190320145410

[45] A. Nagai, A. Takahashi, T. Komatsu, T. Nakagawa, Complex formation of poly(4-vinylpyridine) with copper(II) ion in mixed solvent, Polym. J. 20 (1988) 609–614. DOI: 10.1295/polymj.20.609

[46] T. Zheng, Mo Zhu, M. Waqas, A. Umair, M. Zaheer, J. Yang, X. Duan, L. Li, P4VP-RuII(bda) polyelectrolyte–metal complex as water oxidation catalyst: on the unique slow-diffusion and multi-charge effects of the polyelectrolyte ligand, RSC Adv. 8 (2018) 38818-38830. DOI: 10.1039/c8ra08012g

[47] E. Hobbollahi, M. List, U. Monkowius, Poly(4-vinylpyridine) as ligand for Au(I) and Zn(II) cations: luminescent metal-containing polymers, Monatsh. Chem. 150 (2019) 877–883. DOI: 10.1007/s00706-019-2382-4